Preformulation screening of lipids using solubility parameter concept in conjunction with experimental research to develop ceftriaxone loaded nanostructured lipid carriers

Swarupanjali Padhi[1*], Rupa Mazumder[1], Shradha Bisht[2]

[1]Department of Pharmaceutics, Noida Institute of Engineering and Technology (Pharmacy Institute), Greater Noida, Uttar Pradesh, India, [2]Department of Pharmacology, Amity Institute of Pharmacy, Lucknow Amity University, Uttar Pradesh, India

Development of ceftriaxone loaded nanostructured lipid carriers to increase permeability of ceftriaxone across uninflamed meninges after parenteral administration. Lipids were selected by theoretical and experimental techniques and optimization of NLCs done by response surface methodology using Box-Behnken design. The $\Delta\delta t$ for glyceryl monostearate and Capryol90 were 4.39 and 2.92 respectively. The drug had maximum solubility of 0.175% (w/w) in glycerol monostearate and 2.56g of Capryol90 dissolved 10mg of drug. The binary mixture consisted of glyceryl monostearate and Capryol90 in a ratio of 70:30. The optimized NLCs particle size was 130.54nm, polydispersity index 0.28, % entrapment efficiency 44.32%, zeta potential -29.05mV, and % drug loading 8.10%. *In vitro* permeability of ceftriaxone loaded NLCs was 5.06×10^{-6} cm/s; evidently, the NLCs pervaded through uninflamed meninges, which, was further confirmed from *in vivo* biodistribution studies. The ratio of drug concentration between brain and plasma for ceftriaxone loaded NLCs was 0.29 and that for ceftriaxone solution was 0.02. With 44.32% entrapment of the drug in NLCs the biodistribution of ceftriaxone was enhanced 7.9 times compared with that of ceftriaxone solution. DSC and XRD studies revealed formation of imperfect crystalline NLCs. NLCs improved permeability of ceftriaxone through uninflamed meninges resulting in better management of CNS infections.

Keywords: PAMPA-PBL. X-ray diffraction. Imperfect crystalline. The full width half maximum. Solubility parameter.

INTRODUCTION

The challenge associated with the delivery of drugs to central nervous system (CNS) is to surmount the problem of permeability through different barriers like blood brain barrier, blood-cerebrospinal barrier, and the different efflux system (Santaguida *et al.*, 2006; Huttunen, Rautio, 2011). In case of CNS infections these barriers act peculiarly, the meninges inflame during the peak infection and the distorted meninges allows the free passage of

the xenobiotics. The problem arises when the infection is on the verge of cure, the meninges start to repair itself and become uninflamed, hindering the penetration of antimicrobial drugs, resulting in drug resistance (Nau *et al.*, 1993; Emmerson *et al.*, 1985). This problem can be solved by increasing the amount of drug administration, but this may result in toxic side effects.

Ceftriaxone sodium is hydrophilic in nature and enlisted under the cephalosporin class of antibiotic, mainly used as a drug of choice for childhood diseases and bacterial meningitis for susceptible microorganisms (Mandell, Sande, 1996). When the infection is on the approach to cure, the meninges become uninflamed impeding the access of antimicrobial drugs to the brain. Therefore, due to low concentration of drug in

*Correspondence: S. Padhi. Noida Institute of Engineering and Technology (Pharmacy Institute). Greater Noida, Gautam Buddha Nagar, Uttar Pradesh, 201306, India. E-mail: swppadhi@gmail.com. Phone: 7011164903. ORCID: https://orcid.org/0000-0003-2200-5542 | Swarupanjali Padhi: https://orcid.org/0000-0003-2200-5542 | Rupa Mazumder: https://orcid.org/0000-0002-1888-548X | Shradha Bisht: https://orcid.org/0000-0001-7500-766X

cerebrospinal fluid (CSF) during uninflamed meninges cannot act against moderately or resistant bacterial infection, hence the dose has to be increased to maintain the minimum inhibition concentration of drug (Cherubin et al., 1989), which, may otherwise lead to multi-drug resistance leading to failure of the treatment strategy. The difficulty of ceftriaxone in the current formulation (solution) in crossing BBB is well known (Nau et al.,1993). This restriction associated with ceftriaxone solutions has lead the researchers to reformulate it into such a formulation which allow the drug permeation through uninflamed meninges. As the uninflamed meninges are highly lipophilic in nature and the drug was hydrophilic in nature so it was necessary to design a lipophilic carrier having sufficient space to entrap and enhance the permeability of hydrophilic drug.

Nanostructure lipid carriers (NLCs) may be a suitable dosage form that improves the penetration of the therapeutic agent across the blood brain barrier (BBB) by influencing the tight junction or by the endocytosis process (Padhi, Mazumder, Bisth, 2019; Salunkhe, et al., 2015). NLCs enhances the retention time of drug and maintain its required concentration in the brain for effective and rational treatment of infectious diseases of CNS.

Lipid nanoparticles comprised of solid lipid nanoparticles and nanostructured lipid carriers belonging to first and second generation respectively (Tajes et al., 2014; Gartziandia et al., 2015; Almousallam, Moia, Zhu, 2015) The solid lipid nanoparticles (SLN) is mainly composed of biodegradable solid lipids whereas NLCs had liquid lipids in addition. The incorporation of a small amount of liquid lipids in solid lipids results in the formation of the imperfect crystalline structure of NLCs, which in turn increases its drug loading capability compared to SLN which has crystalline and rigid structure (Neves, Queiroz, Reis, 2016). Therefore, NLCs are suitable for carrying both hydrophilic and lipophilic drugs (Kasongo et al., 2011; Kasongo, Müller, Walker, 2012)

The purpose of this research is to develop parenteral nanostructured lipid carriers of ceftriaxone sodium to enhance the permeability of the same, thus increasing the delivery of the drug to CNS. NLCs carriers due to their lipophilic nature can easily cross the BBB and are able to deliver the hydrophilic drug to the brain. Preformulation studies were carried out to select the suitable solid lipid and liquid lipid. Ceftriaxone loaded NLCs were formulated and optimized using Box Behnken design. *In vitro* permeability studies were carried out by using parallel artificial membrane permeability assay and biodistribution studies in rat's brain were performed. X-ray diffraction and thermal analysis gave the structural interpretation of the optimized formulation (Shah et al.,2019).

MATERIAL AND METHODS

Ceftriaxone (disodium salt) was obtained as a gift sample from Cipla limited, Himachal Pradesh (India). Solid lipids glyceryl monostearate (58 to 59^{0}C), Stearic acid (MP: 67to72^{0}C), Oleic Acid, Isopropyl myristate, and Tween 80 were obtained from CDH Pvt. Ltd. Compritol 888 pellets (69-74^{0}C), Precirol ATO 5(52-56^{0}C), Capryol90 (propylene glycol monocaprylate) Lauroglycol FCC(propylene glycol monolaurate (TypeI)), Labrafac PG (propylene glycol dicaprylate /dicaprate) gifted by Gattefosse India Pvt. Ltd., Softisan 154 (53-58^{0}C), Imwitor 900(F)P (54-64^{0}C), Miglyol 812N (Caprylic/ Capric Triglyceride) were gifted by IOI Oleo GmbH. Porcine Polar Brain Lipid (PBL) was obtained from Sigma Aldrich, India. Distilled water was prepared using a double distillation unit. All other ingredients used were of analytical grade and purchased from CDH Pvt. Ltd. India.

Preformulation studies

In this study, theoretical and experimental solubility were conducted to find suitable lipids for the preparation of NLCs. Then the binary mixture ratio of both the solid lipids and liquid lipids was selected based on the differential scanning calorimeter (DSC) studies. Fourier transform infrared (FTIR) studies and thermal analysis were conducted to interpret the compatibility between the lipids and the drug.

Determination of solubility parameter

Solubility of the drug in different lipids was determined using both theoretical and experimental

methods. The excipients (lipids) used for such formulations are expensive and screening these lipids by experimental approaches are exhaustive, costly, and time-consuming. So, researchers have adapted more rational methods like solubility parameters which account for the cohesive energy density of components and were determined by the group contribution method (Hancock, York, Rowe, 1967; Barra *et al.*, 1997).

Theoretically, the determined solubility parameter of the ingredient is a fast-screening tool for the selection of lipid candidates (Hancock, York, Rowe, 1967; Krevelen, 2009; Lakshmi *et al.,* 2009). It is considered that if (total solubility parameter of drug minus total solubility parameter of lipids) $\Delta\delta_t \leq 5$ then the drug will be miscible in the excipient to a greater extent (Krevelen, 2009; Hansen, 1967). To accord, the theoretical results with experimental results, partition co-efficient of drug between lipid and aqueous phase and solubility between drug and lipids were performed.

Calculation of total solubility parameters:

Hansen introduced the measurement of the cohesive energy of a substance by measuring the total solubility parameter (δ_t) (Rowe, 1998). The calculation was done based on specific interatomic or intermolecular forces of attraction between a solvent and a solute. The total solubility parameter consists of three factors.

$$\delta_t^2 = \delta_d^2 + \delta_p^2 + \delta_h^2 \tag{1}$$

where δ_t, δ_d, δ_p, δ_h stands for total solubility parameter, partial solubility parameter associated with dispersion force, partial solubility parameter associated polar force, and partial solubility parameter associated hydrogen bonding respectively. Moreover, the solubility of a given polymer in different solvents depends on its chemical structure. Structural similarity favors solubility; hence, it is required to have comprehensive information regarding the chemical structure of the substance. Different researchers like Smalls, Van Krevelen, Hoys, Fedors, and others have suggested methods of group contributions that can be used

to find the different forces between the solvent and solute. In this study, the Van Krevelen method of group contribution has been used.

$$\delta_d = \frac{\Sigma F_d}{\Sigma V} \tag{2}$$

$$\delta_p = \frac{\sqrt{\Sigma F_p^2}}{\Sigma V} \tag{3}$$

$$\delta_h = \sqrt{\frac{\Sigma E_h}{\Sigma V}} \tag{4}$$

Here F_d, F_p, E_h stands for the group contribution to dispersion forces, polar forces, hydrogen bond energy respectively and V is the molar volume.

Likewise, the mixing enthalpy (ΔH_M) per unit volume between compound 1 and compound 2 becomes:

$$\Delta H_M = \varphi_1 \varphi_2 [(\delta_{d_1} - \delta_{d_2})^2 + (\delta_{p_1} - \delta_{p_2})^2 + (\delta_{h_1} - \delta_{h_2})^2] \tag{5}$$

Here φ_1 and φ_2 are the volume fractions of component 1 and component 2, respectively.

The polarity of a substance (Xp) gives an account of the contribution of hydrogen bonding and other polar interactions (Li *et al.*, 2006).

$$X_p = 1 - \frac{\delta_d^2}{\delta_{total}^2} \tag{6}$$

In the current study, partial and total solubility parameters and polarity of a total of 12 lipids and the drug ceftriaxone sodium were calculated using Eq. (1), (2), (3), (4), and (6), with the values of F_d, F_p, E_h, and V of specific functional groups being obtained from the literature. The enthalpy of mixing between the lipids and the complex was calculated using Eq. (5)

The calculated values of three partial solubility parameters, the total solubility parameter and polarity of 12 lipids, and the drug ceftriaxone were obtained to further calculate the differences in the partial

solubility parameters, total solubility parameters, and polarity between the drug ceftriaxone and the lipids. The structure of the drug is given in Figure 1 Mixing enthalpy (ΔH_M) between the drug and lipids was calculated to estimate the amount of energy required to attain mutual solubility between the drug and lipids. For the calculation of solubility parameters for a polymeric moiety, single repeating monomer units were considered and for the lipids comprising of a mixture of glycerides estimated on an average of the main ratio (Shah, Agrawal, 2013).
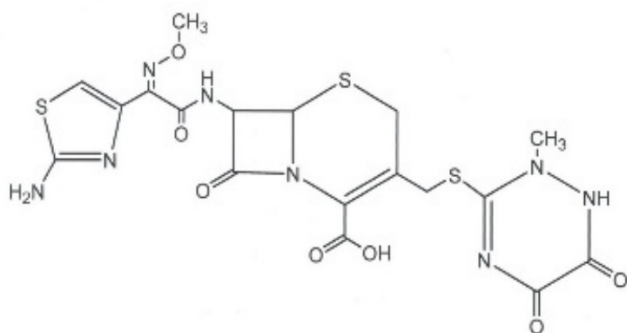
FIGURE 1 - Structure of ceftriaxone.

Determination of solubility of the drug in solid lipids and liquid lipids

0.025% (w/w) of ceftriaxone was blended with solid lipid and the mixture was heated at 85^0C and agitated at 100rpm using a rotary incubator for 24h. Solubility of the drug in the molten lipid was visually assessed. The concentration of the drug in the lipid was added step wise by 0.025% (w/w) until ceftriaxone sodium particle remain undissolved in molten lipid after 24h (Kasongo *et al*., 2011)

The solubility of ceftriaxone in liquid lipid was determined by taking 10mg of drug in a wide mouth screw capped bottle, to which, preheated liquid lipid was progressively added and continuously stirred on a magnetic stirrer. The development of a clear, pale yellow solution of liquid lipid indicated the endpoint of the solubility study. The volume of liquid lipid essential to solubilize the drug was determined (McDaid *et al.,* 2003). All the readings were taken in triplicate.

Partition coefficient measurement of the drug in different lipids

10mg of ceftriaxone sodium was dispersed in a blend of 1g of molten lipid and 1ml of double distilled water and the same was maintained at 5^0C above the melting point of the lipid. The combination was stirred at the same temperature for 45 min and then, kept undisturbed for 1h, allowing the partition to reach equilibrium. The aqueous phase was collected after cooling and was analyzed for ceftriaxone content using a UV spectrophotometer (UV 1700, Shimadzu, Japan) at 266nm wavelength (McDaid *et al.,* 2003). All the readings were taken in triplicate.

Selection of a binary mixture of solid and liquid lipid

The solid and liquid lipid with which the drug had the best solubility were mixed in different ratios of 90:10, 85:15, 80:20, 70:30, 60:40, 50:50. The lipid mixtures were stirred at 1200rpm for 2h at 85^0C rotary incubator shaker. Then for 24h, the samples were kept at room temperature before the samples were sent for differential scanning calorimetry (DSC) analysis. Samples weighing between 1 to 2mg were taken and the DSC was run from 0^0C to 100^0C temperature. The heating rate of the pans was regulated at 10^0C/min. The miscibility of the two lipids was also checked by smearing a cooled sample of the mixture on a hydrophilic filter paper to determine the presence of any oil droplets on the hydrophilic filter paper. The absence of any oil droplets and the width of the thermal event along with crystallinity was considered for developing ceftriaxone loaded NLCs (Kasongo *et al*., 2011).

Compatibility testing between drug and lipid excipient

For compatibility studies, FTIR of pure drug, both the solid lipids, liquid lipids, and mixture of drug and lipids were conducted, respectively. The FTIR curves of pure components were compared to the curves obtained from the physical mixture (1 part of drug and 1 part of a binary mixture of lipids) kept at room temperature for three months. The mixture of the lipid consists of the blend of solid lipid and liquid lipid in the ratio

selected by the thermal event studies. FTIR spectra of lipid and drug were recorded on a Perkin Elmer, FTIR spectrophotometer model, within the range of 4000–400cm^{-1} at a scanning rate of 4mm/s and at a resolution of 2cm^{-1} using KBr disc as reference. Similarly, the samples were prepared for thermal analysis (DSC), 131 EVO. 2 mg of each sample was weighed, and the instrument ran from 0^{0}C to 180^{0}C temperature and the rate of heating of the pans were regulated at 10^{0}C/min (Pani *et al.*, 2012).

Experimental design and statistical analysis

Preliminary experiments were conducted before selecting the factors for the development of the experimental model for optimization. For this experiment, two response surface designs could have been employed, like central composite design (CCD) and Box-Behnken design (BBD) to develop suitable polynomial models to be used for optimization. In the present study, Box-Behnken design was preferred over CCD, as in the former, it requires fewer runs compared to the latter with 3 or 4 variables. The BBD helped to predict the parameters of a quadratic model and avoided experiments involving a simultaneous combination of extreme levels of all factors as it was represented by a multidimensional cube and a central point, in which the experimental points were located at the midpoint of each side of the cube. In Box Behnken design with 3-factors, 3-levels, and 3 central points, experiment for 1 block (15 experimental runs) was used to determine the first and second order coefficients of the mathematical model used. BBD was built up using a statistical software Stat-ease (Design Expert) considering three independent variables like the total amount of lipids (A), speed of homogenization (B), and concentration of surfactant (C) and three dependent variables at 3 levels for each factor (Table I). Fifteen formulations were prepared, and their responses found were filled in the design matrix (Table II). The fifteen formulations were replicated twice. The effect and interaction between the various factors were determined and the polynomial equation giving rise to the optimum model was obtained. The validation of the polynomial equation was also tested (Mahdi *et al.*, 2021; Mohammed *et al.*, 2021; Jayanthi *et al.*, 2016; Park *et al.*, 2019; Patil, Surana, 2013).

TABLE I - List of independent factors considered at different levels and the dependent variables with desired constraints

Independent variables	Levels		
	-1	**0**	**1**
A= Total amount of lipid (mg)	200	300	400
B= homogenization speed(rpm)	10000	12000	14000
C= concentration of surfactant (%)	1	1.5	2
Dependent variables	**Constraints**		
Y_1=Entrapment efficiency (%)	Maximum		
Y_2= Particle size(nm)	Minimum		
Y_3= Zeta Potential(mV)	Maximum [*]		

*Gonzalo *et al.,* 2018.

Y= β$_{0+}$ β$_1$A+ β$_2$B+ β$_3$C+ β$_4$AB+ β$_5$AC+ β$_6$BC+ β$_7$A^2+ β$_8$B^2+ β$_9$C^2

Y= response, β$_{0=}$ Arithmetic means of 3 responses

β$_1$, β$_2$, β$_3$, β$_4$, β$_5$, β$_6$, β$_7$, β$_8$, β$_9$= Estimation co-efficient for the corresponding factors A, B, C AB, AC, BC, A^2, B^2, C^2.

TABLE II - Box Behnken experimental design depicting the independent variable and dependent variable

RUNS	INDEPENDENT VARIABLES			DEPENDENT VARIABLE							
				Observed value± SD			Predicted value				
	$A=$ Total amount of lipid (mg)	$B=$ homogenization speed(rpm)	$C=$ concentration of surfactant (%)	Y_1 (particlesize nm)	Y_2 (% entrapment efficiency)	Y_3 (zeta potential, mV)	Y'_1 (particlesize nm)	Y'_2 (% entrapment efficiency)	Y'_3 (zeta potential, mV)	PDI(poly dispersion index)	% Drug loading
F1	-1	-1	0	189.8±2.9	18.9±7.6	-24.4±2.7	182.23	18.24	-24.67	0.27	5.86
F2	+1	-1	0	178.0±3.4	45.0±8.9	-27.9±1.8	175.65	45.65	-28.20	0.34	8.26
F3	-1	+1	0	139.8 ±3.7	19.6±7.2	-26.5±2.9	142.16	18.52	-26.20	0.42	6.08
F4	+1	+1	0	168.7± 2.8	46.9±2.8	-28.6±3.2	176.28	47.08	-28.32	0.31	8.63
F5	-1	0	-1	180.0±5.4	19.5±2.5	-25.3±4.5	178.58	18.75	-25.21	0.38	6.05
F6	+1	0	-1	177.5± 6.8	45.9 ±5.7	-26.8±2.5	178.38	46.95	-26.68	0.33	8.45
F7	-1	0	+1	93.9 ±8.6	18.5 ±6.3	-24.8± 5.2	98.63	18.95	-24.91	0.35	5.88
F8	+1	0	+1	124.9± 4.7	47.8± 7.4	-29.0± 5.4	126.33	48.56	-29.08	0.21	8.75
F9	0	-1	-1	198.7 ±6.5	30.6±6.4	-26.2±2.9	207.70	31.45	-26.11	0.29	7.06
F10	0	+1	-1	186.0 ±7.7	31.5±6.8	-25.7±2.5	185.05	31.67	-26.08	0.43	7.23
F11	0	-1	+1	137.8± 7.9	32.0±9.5	-26.4±3.8	138.75	32.87	-26.31	0.32	7.31
F12	0	+1	+1	124.0 ±5.3	29.3 ±7.8	-28.1±2.9	122.00	29.68	-27.98	0.25	6.72
F13	0	0	0	145.0 ±7.5	29.5± 6.5	-28.5±2.8	144.66	28.98	-28.53	0.41	6.83
F14	0	0	0	147.0 ±6.8	29.9 ±6.7	-28.7 ±1.7	144.66	29.97	-28.53	0.42	6.89
F15	0	0	0	142.0 ±7.8	30.0±6.4	-28.4 ±2.6	144.66	29.86	-28.53	0.39	6.79

Preparation of NLC

NLCs were prepared by hot homogenization method using solid lipid: liquid lipid in a ratio of 70:30. The lipids were melted at 80^0C and 90mg of drug was added to the transparent oily phase. The oil phase was transferred to the aqueous phase (double distilled water + surfactant (Tween 80)) preheated at 80^0C and agitated at 1200 rpm for 15min leading to the formation of primary emulsion, which, was further subjected to high shear homogenization (T 25 digital ULTRA-TURRAX®., Germany) at 10,000-14000rpm for 2.5h. The nano-dispersions were cooled to room temperature and filtered and subjected to lyophilization. (Tsai *et al*., 2012; Hao *et al.,* 2011).

Preparation of lyophilized optimized NLCs

The optimized formulation was prepared as per the different values of independent factors suggested by the optimization method. 5%(w/w) of mannitol was used as a cryoprotectant in the preparation of freeze-dried NLCs because the presence of cryoprotectant would help in the redispersion of lyophilized powder ensuring the formation of nanodispersion and increase the stability of the preparation. Further evaluations were done using freeze-dried preparations.

Determination of particle size and surface morphology, polydispersity index, and zeta potential of prepared NLCs

Dynamic light scattering technique was used to measure the particle size and polydispersity index (PDI) of the nanostructured lipid carrier formulation using Malvern Panalytical, Zetasiser Ver. 7.13, measuring particle sizes ranging from 0.3nm - 10µm. SEM (Verios 5 XHR SEM, Thermo Fisher Scientific, USA) was used to determine the surface morphology as well as the particle size. Zeta potential was also measured simultaneously using electrophoretic light scattering technique measuring electrophoretic mobility of particles in formulation. Preceding to measurements, all the illustrations were diluted with distilled water and all the measurements were carried out in triplicate (Feng *et al*., 2011; Alam *et al.,* 2015; Ameeduzzafar *et al*., 2019).

Determination of % entrapment efficiency (EE) and % drug loading(%DL)

The amount of drug entrapped in the lipid matrix was determined by centrifuging the prepared NLCs at 15,000rpm for 30mins at 25^0C, followed by the estimation of the amount of drug remaining in the supernatant by UV spectrophotometer at 266nm (UV 1700, Shimadzu, Japan).

EE was calculated using the following formula:

$$\%EE = \frac{w_1-w_2}{w_1} X100 \qquad (1)$$

$$\%DL = \frac{w_1-w_2}{w_{1+w_3}} X100 \qquad (2)$$

Where, w_1, w_2, w_3 represented the weight of the drug in formulation, the weight of the drug in the supernatant, and weight of lipids, respectively (Salem *et al*., 2018; Li *et al*., 2008; Subedi, Kang, Choi, 2009).

In vitro drug release study

The dialysis bag method was used for *in vitro* drug release analysis and the experiment was performed in pH

7.4 phosphate buffer using dialysis membrane (12,000-14,000 molecular weight cut-off). The dialysis tube was first cleaned with warm double distilled water and one end of the dialysis tube was tied, 50mg equivalent drug of lyophilized NLCs was dispersed in 2ml of sterile water was poured into it and the other end was also closed. The dialysis tube was immersed in 200ml of dissolution medium and constantly stirred at 37^0C temperature at 100 rpm. 2ml aliquots were withdrawn at different predetermined time intervals and substituted by an equal volume of a fresh dissolution medium. The sample after appropriate dilution were spectrophotometrically examined at 266nm (Shah *et al*., 2012; Ameeduzzafar, Qumber, Alruwaili, 2021)

In vitro permeability studies using parallel artificial membrane permeability assay

PAMPA was performed using Porcine Polar Brain Lipid (PBL) which resembles the BBB, was used to study the permeability of ceftriaxone-loaded NLCs. Porcine Polar Brain Lipid was dissolved in n-dodecane to obtain the solution of (2%w/v) concentration. 96 well filter plate was employed for experimental determination of permeability. PBL (5µl) was added to the filter paper attached to the donor chamber. A sandwich arrangement was followed with an acceptor at the bottom and a donor compartment at the top with the filter paper in between them. 300µl (containing 150µg equivalent drug) of drug solution or formulation of NLCs were added to the donor compartment and the acceptor compartment was filled with phosphate buffered solution of pH 7.4. After incubating for 0.5h, 2h, 4h, 6h, and 10h samples were withdrawn from the acceptor chamber at a specified time interval and replaced with a fresh medium. 150µl of the NLCs formulation was withdrawn from acceptor compartment and diluted with 50µl acetonitrile and placed in the ultrasonic bath for 30min, and finally ultra-centrifuged for 3min at 13000rpm at room temperature. The concentration of drug was detected by ultra-fast liquid chromatography (UFLC). Similar steps as above are followed for the drug solution.

Permeability of ceftriaxone loaded NLCs formulation and drug solution of ceftriaxone through

PAMPA-BBB after incubating it for 10h, was calculated using the following formula (Graverini *et al.,* 2018; Ameeduzzafar, 2020).

$$Pe = -\ln[1 - CA(t)/ Cequilibrium]/A \times (1/VD + 1/VA) \times t$$

where Pe is permeability (cm/s), A = effective filter area, VD = donor well volume (ml), VA = receptor well volume (ml), t = incubation time (s), CA(t) = compound concentration in receptor well at time t, CD (t) = compound concentration in donor well at time t, and

$$Cequilibrium\ (t=0) = [CD(t) \times VD + CA(t) \times VA]/(VD + VA)$$

Experiments were performed in triplicate and the mean of three samples was used for data analysis.

Biodistribution studies

The experimental animals were kept as per the ethical guidelines (CPCSEA) and the permission for the use of Wistar rats was given by the ethical committee of Noida Institute of Engineering and Technology (Pharmacy Institute), Greater Noida, India (Protocol number: IAEC/NIET/2018/01/01) to collect the brain and plasma from the rats after sacrificing them by cervical dislocation. Male Wistar rats were selected and divided into two groups. One group (n=4) was injected ceftriaxone loaded NLCs (dose equivalent to 50mg/Kg) intravenously through the tail vein and the other group (n=4) was administered ceftriaxone solution (dose equivalent to 50mg/Kg) through IV via tail vein. After 8h the brain was removed by opening the skull and washed and weighed before extraction of the drug. 500µl of water was added to 0.5g of brain tissue, homogenized and then 100µl of acetonitrile was added to it. These samples were subjected to centrifugation at 13000rpm for 3min at room temperature and the supernatant was removed, filtered using 0.22µm filter paper, and 20µl sample was injected into the UFLC system. Similarly, 1ml of blood sample was collected and to this 300µl of acetonitrile added and centrifuged at 13000rpm for 3min at room temperature and the supernatant was separated and filtered using

0.22µm filter paper, and 20µl sample was injected into the UFLC system.

A prominence UFLC Shimadzu system was used, which, has a UV-Vis detector, C18G (250mm x 4.6mm id and particle size 5µm) sample injection loop was employed. The Shimadzu LC solution software was used to regulate and assimilate the output signals. The flow rate was maintained at 1ml/min in isocratic mode and the run time was fixed for 15mins. The detector was set at 266nm. The mobile phase consisting of phosphate buffer and acetonitrile were mixed in a ratio of 70:30% v/v, respectively, and ion-pairing agent 5mM (N-cetyl N, N, N- trimethyl ammonium bromide) with pH 8.0 was used as the mobile phase.

Structural characterization of Lyophilized NLCs formulation

The structural characterization was carried out by thermal analysis and X-ray diffraction examination to study the arrangement of the drug in the lipid matrix.

Differential scanning calorimetry

The thermal behavior of drug, solid lipid, physical mixture of solid lipid, liquid lipids, and drug and lyophilized formulation of the prepared NLCs were measured using differential scanning calorimeter (DSC), 131 EVO. 2 mg of each sample was weighed, and the instrument ran from 0°C to 180°C temperature. The rate of heating of the pans was regulated at 10°C/min (Kovacevic *et al*., 2011).

X-ray diffraction

An X-ray diffractometer (Ultima IV, Rigaku, Japan) with a Scintillation counter and K-beta filter, was used to investigate the crystalline structure of the samples like drug (ceftriaxone), solid lipid (glyceryl monostearate), physical mixture of drug, solid lipid, and liquid lipid and freeze-dried ceftriaxone loaded NLCs.

All samples were characterized in their solid form with a scanning rate of 8.00 deg./min. over 2 theta with a scan range of 10 - 80 deg (Eedara *et al*., 2018).

RESULT AND DISCUSSION

Theoretical calculation of solubility parameter of ceftriaxone sodium in lipids

Van Krevelen's group contribution method was applied to determine the solubility of the drug in lipids. The chemical structure formula of 12 lipids given in Table III and the three parts of the solubility parameter were manually estimated. The solubility parameter of ceftriaxone sodium is 25.18 and its polarity is 0.38. Table III shows that the calculated total solubility parameters (δ_t) of solid lipids vary from 18.05 to 20.79 and that of liquid lipids vary from 15.61 to 22.26. Similarly, the polarity (X_p) of the solid lipids varies from 0.07 to 0.31 and that of liquid lipids varies from 0.1 to 0.3. The difference between total solubility parameters of ceftriaxone and various solid lipids range between 4.39 to 7.13 and that of total solubility parameters of ceftriaxone and various liquid lipids range between 2.92 to 9.57 (Table IV). Similarly, the difference in polarity of the drug and various solid lipids varies from 0.07 to 0.31, while the difference in polarity of the drug and various liquid lipids varies from 0.08 to 0.28. It is also clear from Table IV that the mixing enthalpies of drugs with various solid lipids vary from 5.98 to 22.84, while that of drugs and liquid lipids vary from 2.52 to 25.57.

Ceftriaxone is a hydrophilic molecule having low permeability across the biological membrane (especially through the uninflamed meninges) and in this research, the permeability of the drug is enhanced by loading it in lipid nanocarriers. Preceding the incorporation of the drug into the lipid matrix, it is significant to determine its solubility of the drug in the lipid as this has an impact on drug entrapment efficiency. Theoretical and experimental solubility analyses were conducted to find the solid lipid and liquid lipid in which the drug exhibited maximum solubility. The lipids consist of fatty acids of different chain lengths, triglycerides of various structures, and mixtures of glycerol esters. Dispersion forces, hydrogen bonding, and polar forces determine partial solubility. Dispersion forces are due to the presence of alkyl groups, as the aliphatic chain length or branch increases, the polarity of fatty acids decreases from 0.31 to 0.06 while the presence of functional groups like alcohol, ester, ether, and carboxylic acid group play an important role in enhancing polar forces and hydrogen bonding. Triglycerides of corresponding fatty acids have less polarity due to the domination of alkyl groups, while glyceryls in the mono-form (such as glyceryl mono behenate and glyceryl monostearate) possess stronger polarity than their corresponding fatty acids due to stronger hydrogen bonding between molecules. The hydrophilic nature of ceftriaxone with a polarity of 0.38, is attributed to the existence of many polar groups (e.g., ROH, RCOR, RCOOH). Table IV enumerates the variations in the partial solubility parameters, total solubility parameters, and polarity of ceftriaxone and lipids. The amount of energy required to attain mutual solubility between the drug and lipids is obtained by calculating the mixing enthalpy (ΔH_M) between the drug and lipids. Glyceryl monostearate and glyceryl behenate (mono-) were identified as the most suitable solid lipid based on the differences in total solubility parameter and the polarity as well as the mixing enthalpy between the drug and the lipids; similarly, Capryol90 (propylene glycol monocaprylate (Type II) and Lauroglycol FCC (propylene glycol monolaurate (Type I) were identified as the most suitable liquid lipids candidates for loading of the drug ceftriaxone. Glyceryl behenate (mono-) has smaller differences with the drug but as it constitutes only a small portion (15%) of Compritol ATO 888, it seems to be a poor preference for the preparation of NLCs. Similarly, Imwitor 900(F)P contains only 40-50% of Glyceryl monostearate so it cannot be used. So pure glyceryl monostearate was selected as the solid lipid and Capryol90 was selected as liquid lipid. There was a clear association between the partition coefficient determined experimentally with the calculated values of solubility parameters using Van Krevelen's group distribution method.

TABLE III - Calculated values of partial solubility parameters, total solubility parameter, and polarity of various lipids and the drug ceftriaxone

S. No	Compound	δd $(J/cm^3)^{1/2}$	δp $(J/cm^3)^{1/2}$	δh $(J/cm^3)^{1/2}$	δt $(J/cm^3)^{1/2}$	Xp
	Ceftriaxone sodium	19.77	7.2	13.83	25.18	0.38
	Solid lipids					
1	Stearic acid (octadecanoic acid) $CH_3(CH_2)16COOH$	17.78	1.42	5.81	18.76	0.1
2	Compritol 888 pellets					
	40-60% Diesters of behenic acid (glycerly dibehenate) $[CH_3(CH_2)20COOCH_2]_2CHOH$	16.81	1.08	6.57	18.08	0.14
	21-35% triesters of behenic acid (glyceryl tribehenate)	16.71	0.74	4.27	17.27	0.06
	15-23% glyceryl behenate (mono) $CH_3(CH_2)_20COOCH\,CHOHCH_2OH$	17.07	2.02	10.52	20.15	0.28
	Behenic acid $CH_3(CH_2)_{18}COOH$	16.54	1.09	5.1	17.34	0.09
	Average	16.78	1.23	6.61	18.21	0.14
3	Glyceryl mono stearate $(CH_3(CH_2)_{16}COOCH_2CHOHCH_2OH)$	17.31	2.87	11.16	20.79	0.31
4	Imwitor 900(F)P					
	40-50% Glyceryl monostearate $(CH_3(CH_2)_{16}COOCH_2CHOHCH_2OH)$	17.31	2.87	11.16	20.79	0.31
	Glyceryl distearate $(CH_3(CH_2)_{16}COOCH2CHOHCH_2COO(CH_2)_{16}CH_3)$	17.38	2.05	6.82	18.78	0.14
	Average	17.35	2.46	9.21	19.79	0.23
5	Precirol ATO 5					
	Glyceryl palmitostearate $(CH_2COO(CH_2)_{14}CH_3\,(CHOH)CH_2COO(CH_2)_{16}CH_3)$	17.38	2.15	6.9	18.86	0.15
6	Softisan 154					
	(hydrogenated vegetable oils are a mixture of triglycerides of fatty acids $CH_3(CH_2)_{14}COOCH_2CHCOO(CH_2)_{14}CH_3CH_2COO(CH_2)_{14}CH_3$	17.42	1.87	4.32	18.05	0.07
	Liquid lipids					
1	Oleic Acid $(CH_3(CH_2)_6CH_2CH=CHCH_2(CH_2)_6COOH$	17.59	1.43	5.85	18.59	0.1
2	Isopropyl myristate $(CH_3CH(CH_3)COO(CH_2)_{12}CH_3)$	14.74	3.01	4.16	15.61	0.11
3	Capryol 90 (propylene glycol monocaprylate (Type II)) $(CH_3(CH_2)_6COOCH_2CHOHCH_3)$	18.62	4.98	11.15	22.26	0.3
4	Lauroglycol FCC (propylene glycol monolaurate (TypeI)) $(CH_3(CH_2)_{10}COOCH_2CH(OH)CH_3)$	18.32	3.8	9.74	21.9	0.25
5	Labrafac PG (propylene glycol dicaprylate /dicaprate) $((COOH)(CH_2)_{16}COOCH(CH_3)CH_2COO(CH_2)_{16}COOH)$	18.35	2.63	8.92	20.57	0.2
6	Miglyol 812N					

TABLE III - Calculated values of partial solubility parameters, total solubility parameter, and polarity of various lipids and the drug ceftriaxone

S. No	Compound	δd $(J/cm^3)^{1/2}$	δp $(J/cm^3)^{1/2}$	δh $(J/cm^3)^{1/2}$	δt $(J/cm^3)^{1/2}$	Xp
	Glyceryl tricaprylate $CH_3(CH_2)_6 COOCH_2CH(COO(CH_2)_6CH_3) CH_2 COO(CH_2)_6CH_3$	17.45	3.15	5.61	18.59	0.12
	Glyceryl tricaprate $CH_3(CH_2)_8 COOCH_2CH(COO(CH_2)_8CH_3) CH_2 COO(CH_2)_8CH_3$	17.44	2.64	5.13	18.36	0.1
	Average	17.45	2.89	5.37	18.48	0.11

δ_t = total solubility parameter, δ_d= partial solubility parameter associated with dispersion force, δ_p= partial solubility parameter associated polar force and δ_h = partial solubility parameter associated hydrogen bonding, Xp = polarity of various lipids, and the drug ceftriaxone

TABLE IV - The differences of partial solubility parameters, total solubility parameter, mixing enthalpy and polarity between various lipids and drug ceftriaxone

S. No	Compound	$\Delta\delta d$ $(J/cm^3)^{1/2}$	$\Delta\delta p$ $(J/cm^3)^{1/2}$	$\Delta\delta h$ $(J/cm^3)^{1/2}$	$\Delta\delta t$ $(J/cm^3)^{1/2}$	Δxp $(J/cm^3)^{1/2}$	ΔHM (J/cm^3)
	Solid lipids						
1	Stearic acid (octadecanoic acid)	1.99	5.78	8.02	6.42	0.28	19.06
2	Compritol 888 pellets						
	40-60% diesters of behenic acid(glycerly dibehenate)	2.96	6.12	7.26	7.1	0.24	18.55
	21-35% triesters of behenic acid (glyceryl tribehenate)	3.06	6.46	9.56	7.91	0.32	26.72
	15-23%glyceryl behenate (mono)	2.7	5.18	3.31	5.03	0.1	8.45
	Behenic acid	3.23	6.11	8.73	7.84	0.29	23.25
	Average	2.98	5.97	7.215	6.97	0.24	19.24
3	Glyceryl monostearate	2.46	4.33	2.67	4.39	0.07	5.99
4	Imwitor 900(F)P						
	40-50% glyceryl monostearate	2.46	4.33	2.67	4.39	0.07	5.99
	Glyceryl distearate	2.39	5.15	7.01	6.4	0.24	15.26
	Average	2.43	4.74	4.84	5.40	0 .155	10.62
5	Precirol ATO 5						
	Glyceryl palmitostearate	2.39	5.05	6.93	6.32	0.23	14.86
6	Softisan 154 (hydrogenated vegetable oils are a mixture of triglycerides of fatty acids	1.72	5.33	9.51	7.13	0.31	22.84
	Liquid lipids						
1	Oleic Acid	2.18	5.77	7.98	6.59	0.28	19.07

TABLE IV - The differences of partial solubility parameters, total solubility parameter, mixing enthalpy and polarity between various lipids and drug ceftriaxone

S. No	Compound	$\Delta\delta d$ $(J/cm^3)^{1/2}$	$\Delta\delta p$ $(J/cm^3)^{1/2}$	$\Delta\delta h$ $(J/cm^3)^{1/2}$	$\Delta\delta t$ $(J/cm^3)^{1/2}$	Δxp $(J/cm^3)^{1/2}$	ΔHM (J/cm^3)
2	Isopropyl myristate	5.03	4.19	9.67	9.57	0.27	25.57
3	Capryol 90 (propylene glycol monocaprylate (type II))	1.15	2.22	2.68	2.92	0.08	2.52
4	Lauroglycol FCC(propylene glycol monolaurate (Type I)	1.45	3.4	4.09	3.28	0.13	5.69
5	Labrafac PG (propylene glycol dicaprylate /dicaprate)	1.42	4.57	4.91	4.61	0.18	8.81
6	Miglyol 812N						
	Glyceryl tricaprylate	2.32	4.05	8.22	6.59	0.26	16.75
	Glyceryl tricaprate	2.33	4.56	8.7	6.82	0.28	19.11
	Average	2.33	4.30	8.46	6.71	0.27	17.93

$\Delta\delta_t$ = difference between total solubility parameter of drug and lipids, $\Delta\delta_d$ = difference between partial solubility parameter associated with dispersion force of drug and lipid, $\Delta\delta_p$ = difference between partial solubility parameter associated polar force of drug and lipid, $\Delta\delta_h$ = difference between partial solubility parameter associated hydrogen bonding of drug and lipid, ΔXp = difference between polarity of drug and lipid, ΔH_M = mixing enthalpy

Solubility of ceftriaxone sodium in various solid lipids and liquid lipids

The solubility of ceftriaxone sodium in solid lipids and liquid lipids is enumerated in Tables V and VI respectively. As evident from Table V, the drug has low solubility in most of the tested solid lipids. While the drug was found to be having a maximum solubility of 0.175% (w/w) in glycerol monostearate among solid lipids, it had a maximum solubility in Capyrol90 among the liquid lipids.

Polar groups in the glyceryl monostearate facilitate mutual miscibility between glyceryl monostearate and the drug in comparison to other lipids. Glyceryl monostearate and Capryol90 have the best miscibility with ceftriaxone which is evident from the results of the partition experiment and the calculated solubility parameters which corroborated each other.

Solubility data reveals that ceftriaxone has very low solubility in all the solid lipids tested, although, the drug exhibited a comparatively higher degree of solubility in pure glyceryl monostearate. Hence, glyceryl monostearate was selected as the suitable lipid among all the solid lipids investigated. However, if only solid lipid were used then the encapsulation efficiency would have been very low. Therefore, a liquid lipid (Capryol90) was selected in which, the drug had relatively high solubility compared to glyceryl monostearate. The binary mixture of Capryol90 and glyceryl monostearate is likely to have higher encapsulation efficiency than glyceryl monostearate alone.

TABLE V - Solubility of ceftriaxone sodium in various solid lipids

Solid Lipids	Melting Point (oC)	Solubility of Ceftriaxone Sodium							
		0.025% (w/w)	0.050% (w/w)	0.075% (w/w)	0.100% (w/w)	0.125% (w/w)	0.150% (w/w)	0.175% (w/w)	0.200% (w/w)
Glyceryl mono stearate	58- 59	+	+	+	+	+	+	+	-
Imwitor® 900 P	54-64	+	+	+	+	+	+	NA	NA
Precirol® ATO5	52-56	+	+	+	+	+	+	-	NA
Stearic acid	69-70	+	+	+	+	+	+	-	NA
Compritol® 888 ATO	69-74	+	+	+	+	+	-	-	NA
Softisan® 154	53-58	+	+	+	+	+	-	-	NA

Qualitative percentage solubility of ceftriaxone sodium in various molten solid lipid excipients: 'NA' stands for not applicable; '+'denotes soluble and '-' indicates insoluble

TABLE VI - Solubility of ceftriaxone sodium in various liquid lipids

Liquid lipid	Amount of Liquid lipid in (g) required to solubilize 10mg of the drug ± SD
Capryol 90 (propylene glycol monocaprylate (type II))	2.59±0.87
Lauroglycol FCC(propylene glycol monolaurate (Type I)	3.47±0.92
Labrafac PG (propylene glycol dicaprylate /dicaprate)	3.92±0.83
Oleic Acid	4.29±0.95
Miglyol 812N	6.87±0.98
Isopropyl myristate	7.82±1.06

Amount of liquid lipid required to solubilize 10 mg of the drug (ceftriaxone sodium)

Partition coefficient

Partition coefficients (ratio of the concentration of drug in solid lipid to the concentration of drug in aqueous phase) obtained are presented in Table VII. Lipids with monoglyceride of long chain fatty acids (glyceryl monostearate, Imwitor900) and medium chain fatty acids (Capryol90) exhibited the highest partition co-efficient.

TABLE VII - Partition coefficients of the drug in different solid lipids and liquid lipids

S. No	Solid lipids	Apparent partition coefficient ± SD
1	Glycerol mono stearate	0.609 ± 0.05
2	Imwitor 900	0.386 ± 0.04
3	Precirol ATO5	0.282 ± 0.03
4	Stearic acid	0.208 ± 0.03
5	Compitrol ATO888	0.190 ± 0.01
6	Softisan 154	0.183 ± 0.02
S. No	**Liquid lipids**	**Apparent partition coefficient ± SD**
1	Capyrol 90	0.823 ± 0.06
2	Lauroglycol FCC	0.729 ± 0.03
3	Labrafac PG	0.632 ± 0.05
4	Oleic acid	0.544 ± 0.07
5	Mygliol 812N	0.301 ± 0.03
6	Isopropyl Myristate	0.212 ± 0.04

Selection of a binary mixture of solid and liquid lipid

Thermal events like onset, end set, peak of melting temperatures of a binary mixture of glycerol monostearate and Capryol90, taken in different ratios and exposed to heat at 100^0C for 1h. is depicted in Table VIII.

TABLE VIII - DSC parameter for a binary mixture of glycerol monostearate and Capryol90 following exposure to heat at 100^0C for 1h

Glycerol monostearate: Capryol 90	Thermal Event	Onset (0C)	Peak temp (0C)	Enthalpy (J/g)	WME*(0C)	% Crystallinity
100:00	Endothermic	62.29	66.03	103.75	3.74	100
90:10	Endothermic	57.13	61.09	75.05	3.96	72.34
85:15	Endothermic	55.43	59.49	65.83	4.06	63.45
80:20	Endothermic	52.28	57.95	46.46	5.67	44.78
70:30	Endothermic	49.55	56.14	33.78	6.59	32.56
60:40	Endothermic	49.04	52.63	32.31	3.59	31.14
50:50	Endothermic	48.81	52.08	30.53	3.27	29.43

*WME stands for width of melting event

The two lipids were taken in different ratios and subjected to DSC analysis to determine the ratio for the best binary mixture. Results of the DSC studies show that all the binary mixtures exhibit melting points between 45°C to 65°C. Width of the melting events and percentage crystallinity was considered as the parameter for screening the binary mixtures of glyceryl monostearate and Capryol90. The combination of solid lipid and liquid lipid which gave the maximum width of melting events 6.59°C and crystallinity 32.564 % was considered as the best binary mixture. Additional confirmation was done by visualizing no oil droplets of Capryol90 on the filter paper was found, suggesting complete miscibility of 30% Capryol90 in 70% of glyceryl monostearate. But as the concentration of Capryol90 was increased to 40%, it was found that the filter paper was smeared with oil showing that the 40% Capryol90 was immiscible in 60% glyceryl monostearate. From DSC analysis (Table VIII) it was also evident that the peak temperature and the onset temperature of the solid lipid glyceryl monostearate were decreasing with an increase in the concentration of liquid lipid Capryol90.

For the development of NLCs, the specific ratio of glycerol monostearate and Capryol90 was selected based on the thermal event analyzed by DSC, which assesses the ratio at which the solid lipid and the liquid lipid were miscible with each other without oozing out of the liquid lipid from the lipid matrix. The melting point of glyceryl monostearate decreases with the addition of Capryol90. All the binary mixtures showed a melting point above 40°C and the onset and the peak maximum of glyceryl monostearate decreases with increasing concentration of Capryol90 up to 30% (w/w). The width of the melting event increases from 0 to 30% of Capryol90 and at 30% there was a sudden increase in WME and beyond 30% the value of WME decreases. Further, the % crystallinity of glyceryl monostearate was found to decrease with the addition of Capryol90 up to 30% on a further increase of Capryol90 there was not much change in the crystallinity of solid lipid because it was already saturated with the liquid lipid, and it was further confirmed from the smear test that the oil droplets were found when the concentration of Capryol90 was increased beyond 30%. Hence the solid lipid and liquid lipids were taken in a ratio of 70% and 30% respectively. No oil droplets were found on the filter paper for the above-mentioned ratio of lipids.

Compatibility drug-excipient studies by FTIR analysis and DSC

Compatibility of the drug with glycerol monostearate and Capryol90 study was conducted by FTIR method. Figure 2 shows the FTIR curves of the drug with glycerol monostearate and Capyrol90. The mixture of drug and lipids contained all the dips of the functional groups which were present in the drug and both the lipids. So, from FTIR analysis it was confirmed that the drug is compatible with the lipid excipient.
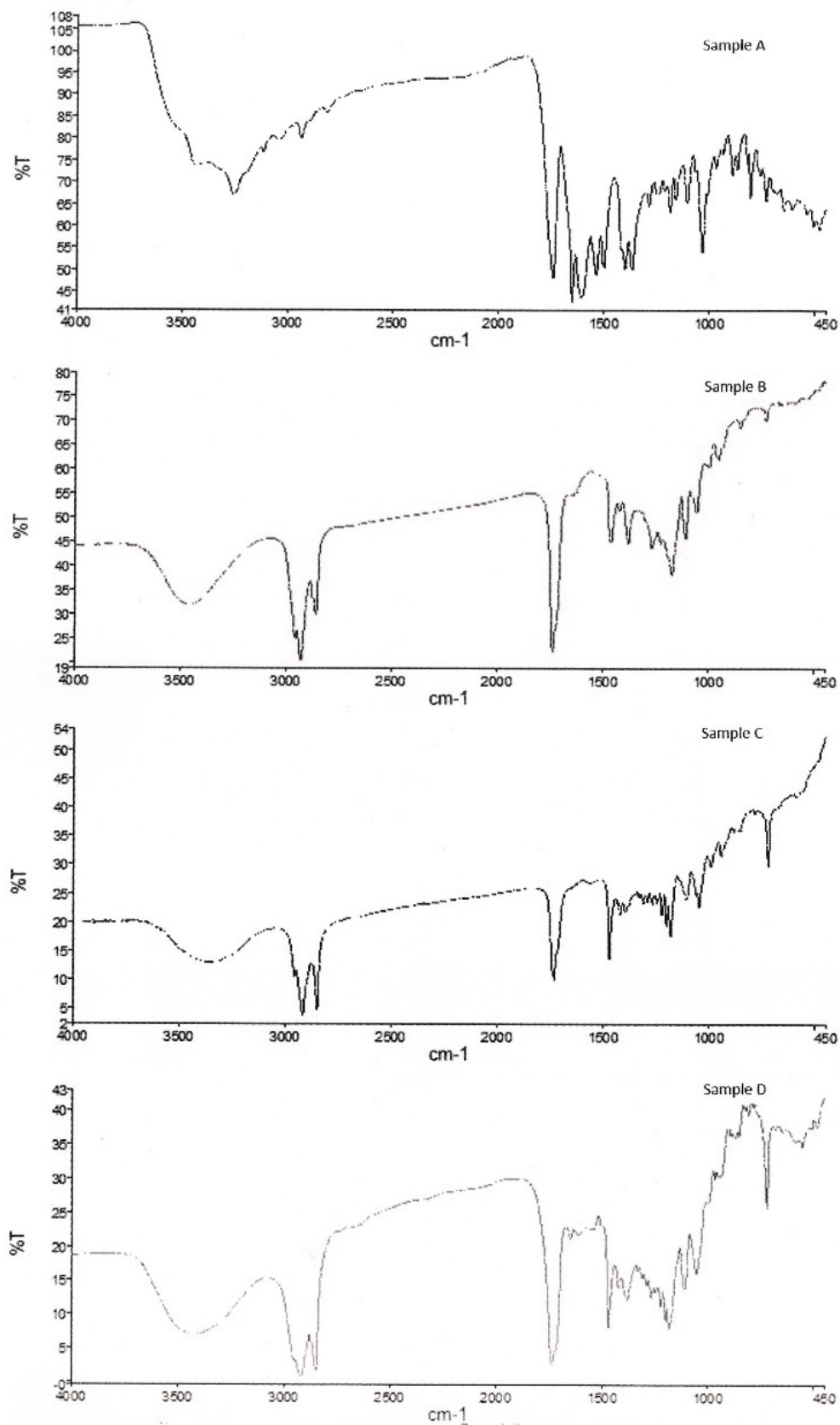
FIGURE 2 - FTIR studies of (A) Ceftriaxone; (B) Glyceryl monostearate; (C) Capryol 90; (D) admixture of ceftriaxone Sodium, glyceryl monostearate, and Capryol 90.

The compatibility studies between the drug and the lipid excipients showed that no new band was obtained for the FTIR analysis of the physical mixture of the drug and the binary mixture of lipids. In pure ceftriaxone these assignments were present viz 3430.95cm^{-1}(asymmetric stretching of (N-H)), 3269.8 cm^{-1} (N-H symmetric stretching), 2936.14cm^{-1}(asymmetric alkane stretching) 1742.08cm^{-1}(beta-lactam C=O stretching), 1605.78cm^{-1}(oxime C-C in ring). In case of Capryol90 3454 cm^{-1} (OH and N-H), 2957.89 cm^{-1}(C-H aliphatic stretching), 1737.96cm^{-1}(C=O aldehyde), 1460.01cm^{-1}(C-H bend alkane), 1418.97cm^{-1} (C-C ring) and for glyceryl monostearate 3899.74cm^{-1}(OH alcohol, phenol), 3361.46cm^{-1}(OH carboxylic acid), 2985.58cm^{-1}(C-H stretch alkane), 1558.44cm^{-1}(nitro compound), 1731.36cm^{-1}(C=O stretching), 1470.86cm^{-1}(C-H bend), 1330.27cm^{-1}(C-N stretching aromatic), 1288.06cm^{-1} (C-H wag). In the case of a physical mixture of drug and lipid excipients, the FTIR assignment showed 3426.11cm^{-1}(N-H stretching), 2956.18cm^{-1}(C-H alkane stretching), 1736.70cm^{-1}(Beta lactam, C=O), 1650.64cm^{-1}(amide stretching), 1611.18cm^{-1}(oxime), 1287.43cm^{-1}(aromatic amine C-N). These assignments belong to the pure drug, or the lipids and no new peaks were formed, therefore it can be concluded that ceftriaxone was compatible with the binary mixture of glyceryl monostearate and Capryol90.

Similarly, the DSC study (Figure 3) showed that the drug has two endothermic peaks, which, are at 65.64°C and 139.7^{0}C and the endothermic peak of solid lipid was at 66.73^{0}C and that of liquid lipid was 39.38^{0}C. The DSC of the physical mixture showed all the peaks of the lipids and the drug viz 66.72^{0}C and 144^{0}C, suggesting that no incompatibility was found between the lipids and drug mixture.
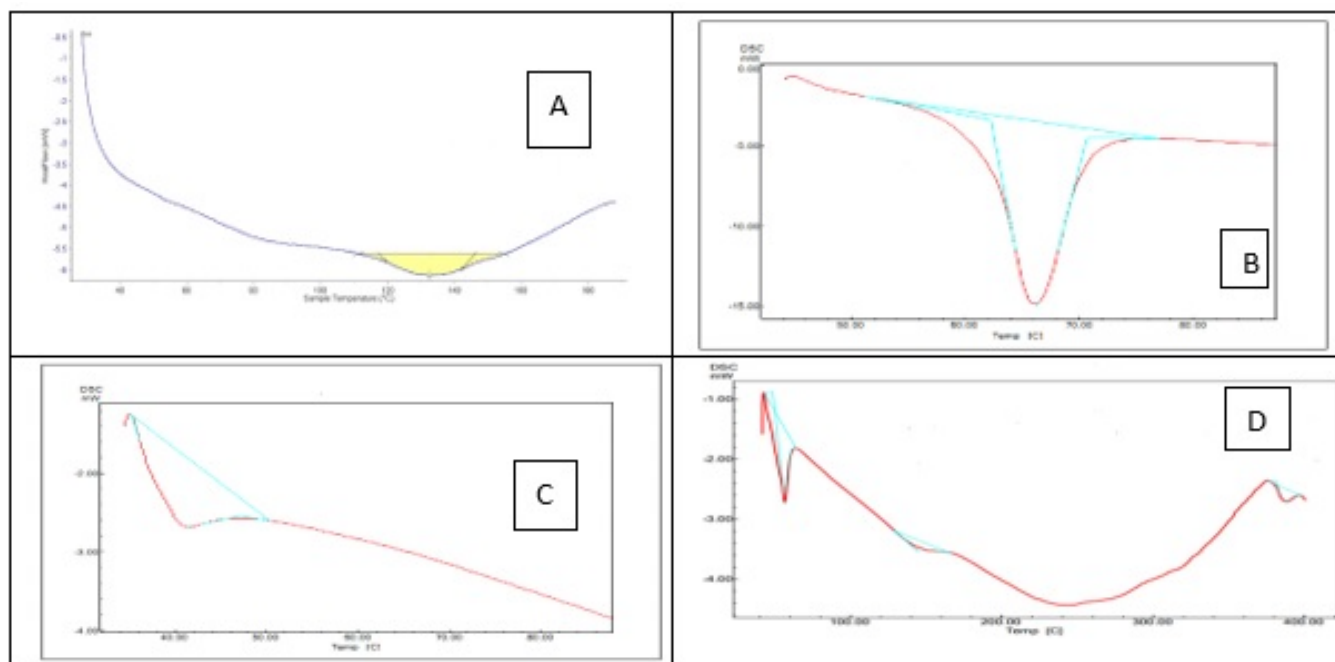
FIGURE 3 - DSC studies of (a) Ceftriaxone; (b) Glyceryl monostearate; (c) Capryol90; (d) admixture of ceftriaxone, glyceryl monostearate, and Capryol90.

Analysis of experimental design

Formulations designed as per Box Behnken design using Design Expert (Stat ease) software have been prepared and evaluated to find the effect of the independent variables, *viz.,* the total amount of lipid, homogenization speed and concentration of surfactant, on the dependent variables, *viz.,* particle size, zeta potential,

and % entrapment efficiency. The significance of the model has been, determined by using ANOVA and it was found that the model was well fitted, and lack of fit was not significant for all the responses (Table IX). The observed value and predicted values of the responses are given in Table II

In this experiment, three residual plots are used to explain adequacy to model and ascertain the assumption of regression. The assumption that the residuals are normally distributed is verified from the normal probability plot of residuals. It is depicted by a straight line. The contours and the 3D response curve were used to analyze the relationship between the independent factors and the interference of factors on the response. After analysis, the three independent factors were optimized to get the desired response (Figure 4).
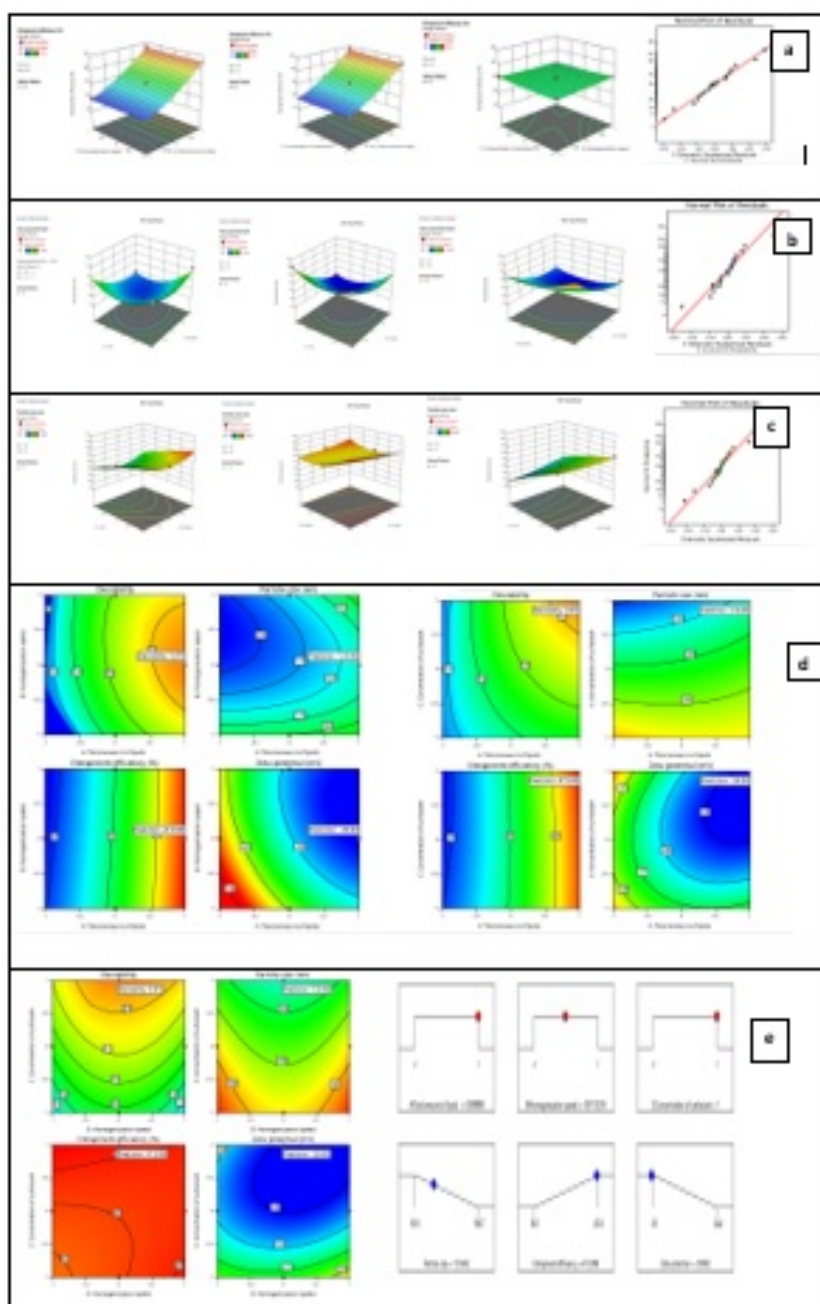
FIGURE 4 - Response surface graphs and Normal plot of residue of (a)Entrapment efficiency, (b) Zeta potential (c) Particle size (d) composite desirability (e) optimized parameters.

The statistical data analysis of experimental work shows that the selected model is significant and the adjusted R^2 value had an excellent agreement with the predicted R^2 value for all the responses considered under investigation. The main aim of this experiment was to increase the permeability of the hydrophilic drug through the uninflamed meninges of the CNS. Therefore, the drug was deceived in nanostructure lipid carriers and the goal of optimization was set at maximum for % entrapment efficiency (EE), maximum (absolute value) for zeta potential, and minimum for particle size. The drug ceftriaxone is entrapped in negatively charged lipids; hence the zeta potential had a negative sign, and stability of the prepared NLCs depends on the magnitude of zeta potential. With the help of Design Expert version 12 software optimal composite desirability of the model was found to be 0.875 suggesting that the selected model would give the desired response. It was found that if the independent variables were secured at 2% concentration of surfactant, homogenization speed at 11868.69 rpm, and the total amount of lipids at 30; mg then it would yield NLCs with a predicted value of % EE equal to 47.68, zeta potential equal to -29.69 mV and particle size equal to 125.46 nm.

TABLE IX - Depicts the model summary and ANOVA (analysis of variance)

Model Summary					
Response	CV%	S	R-sq	R-sq adj	R-sq (predicted)
% Entrapment Efficiency	2.59	0.817	0.99	0.99	0.96
Particle size	4.01	6.23	0.98	0.95	0.76
Zeta potential	1.13	0.306	0.98	0.96	0.79
Analysis of Variance					
Response		Sum of Square	Mean square	F- value	P-value
% Entrapment Efficiency		1514.46	168.27	251.92	0.0001
Particle size		12190.80	1354,53	34.80	0.0006
Zeta potential		32.67	3.63	38.69	0.001
Polynomial Equation					
% Entrapment Efficiency		$30.194 + 13.625\ A + 0.1\ B + -4.05117e\text{-}16\ C + 0.3\ AB + 0.75\ AC + -0.9\ BC + 2.253\ A2 + 0.153\ B2 + 0.503\ C2$			
Particle size		$144.67 + 5.7A - 10.73B - 32.7C + 10.18A\ B + 8.38AC - 0.275\ BC - 3.43\ A^2 - 20.98B^2 - 4.02\ C^2$			
Zeta potential		$-28.53 - 1.41A - 0.5B - 0.5375C + 0.35AB - 0.675AC - 0.55\ BC + 0.9042\ A^2 + 0.7792\ B^2 + 1.15\ C^2$			

S= Standard error; R-sq adj = R-sq adjusted; R^2 (predicted)= predicted R^2 values

Validation of polynomial equation by comparing experimental and predicted value

The variance between the experimental and predicted value was observed to be less than 5%, suggesting that the polynomial equation can be used to predict the responses which can be obtained by altering the quantity of the given set of factors within the given range of value of independent factors (Table X).

TABLE X - Result of validation of polynomial equation

RUNS	INDEPENDENT VARIABLES			DEPENDENT VARIABLE					
				Observed value± SD			Predicted value		
	A= Total amount of lipid (mg)	B = homogenization speed(rpm)	C= concentration of surfactant (%)	Y_1 (Particle size nm)	Y_2 (Entrapment efficiency)	Y_3 (Zeta potential)	Y'_1 (Particle size nm)	Y'_2 (Entrapment efficiency)	Y'_3 (Zeta potential)
FI	220	10000	1.2	200.56±5.6	20.46±2.01	-27.85±2.08	190.41	21.14	-26.74
FII	280	12000	1.6	137.8±4.7	28.65±1.90	-25.85±2.63	134.26	28.89	-26.78
FIII	360	13600	1.8	151.34±3.6	43.89±2.23	-28.43±1.45	140.82	42.10	-29.19

Preparation and evaluation of lyophilized optimized formulation of ceftriaxone loaded nanostructured lipid carrier

After complete analysis, the optimized formulation was prepared using 390mg of lipid, 2% of surfactant, and at 11980 rpm homogenization speed as obtained by optimization method with desirability value close to 1 satisfying all the parameters for optimum performance. The optimized preparation was lyophilized to increase its stability in dry conditions. Mannitol (5%) was used as a cryoprotectant for the lyophilization process. The evaluation of the formulations is given in Table XI. The surface morphology of lyophilized optimized ceftriaxone loaded NLCs analyzed through SEM shows a smooth flattened surface nanoparticle (Figure 5).
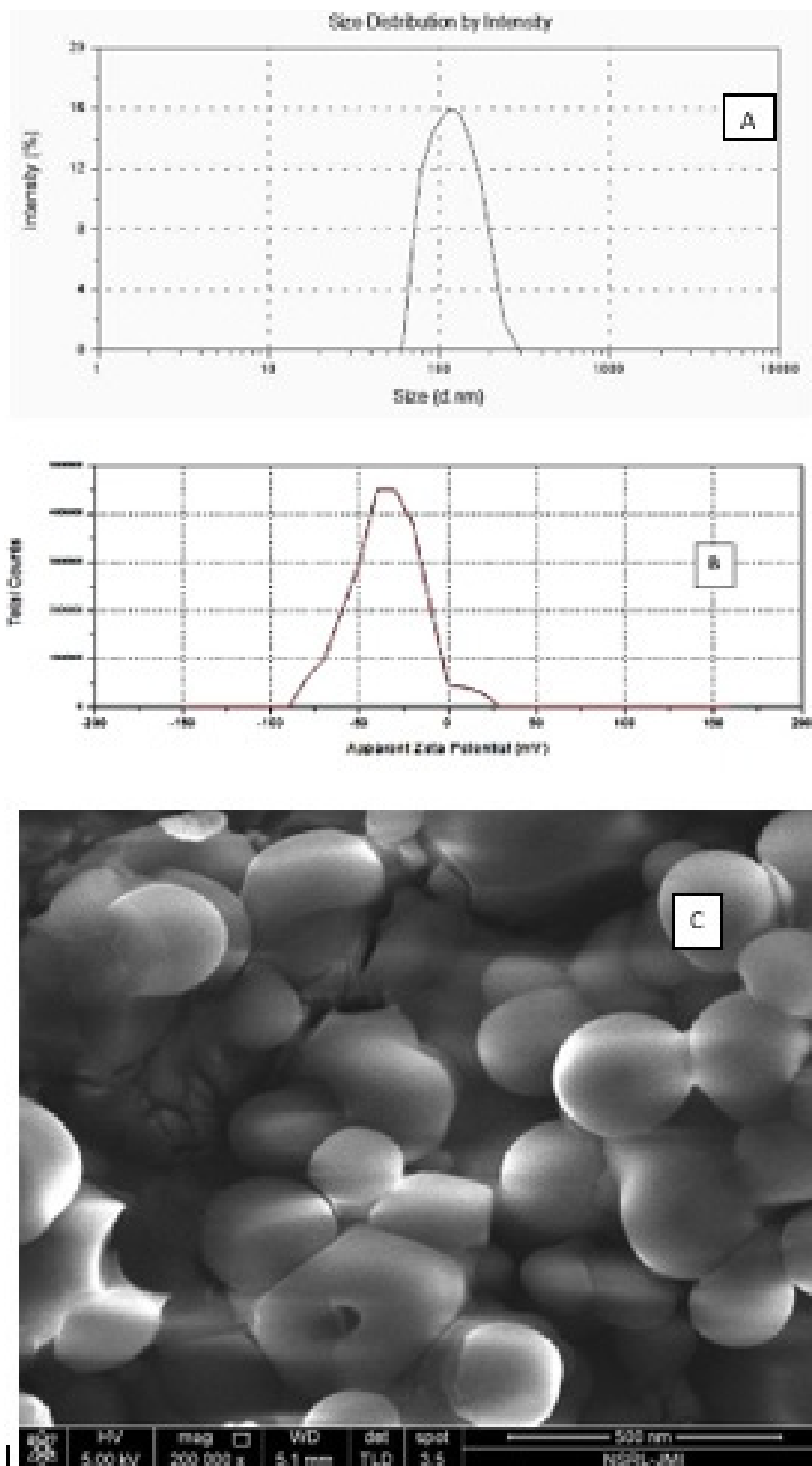
FIGURE 5 - (A) Particle size of lyophilized optimum formulation of ceftriaxone loaded NLCs (B) Zeta potential of lyophilized optimum formulation of ceftriaxone loaded NLCs, (C) SEM surface morphology of lyophilized optimum formulation of ceftriaxone loaded NLCs.

TABLE XI - Evaluation of optimized and lyophilized optimized formulation of ceftriaxone loaded nanostructured lipid carriers

Formulation	Particle Size	PDI	Zeta Potential	% EE	%Drug Loading
Optimized NLCs	126.78nm±6.54	0.26±0.07	-29.14mV±3.47	46.98%±7.48	8.56%±0.86
Lyophilized Optimized NLCs	130.54nm ± 4.7	0.28± 0.089	-29.05mV±4.56	44.32%±5.89	8.10%± 0.8

In vitro release kinetics studies

The lyophilized optimized NLCs formulation exhibited a prolonged release pattern, within 24 h; it showed ~91% of the total drug amount released (Figure 6). The binary mixtures decreased the release of the drug and extended it for more than 24h and ceftriaxone being highly hydrophilic the entrapment achieved was 44% (approximately) only due to the combination of solid lipid and liquid lipid, as the latter distorts the crystalline structure of solid lipid. The release kinetics was found to best fit the slow first order (R^2 =0.97) and Higuchi kinetic model (R^2=0.98), which confirmed that the release followed the diffusion mechanism. Further, when the release data were fitted to the Korsmeyer-Peppas equation it showed that the release exponent (n) was 0.22 which suggested that the release may be due to the Fickian type of diffusion as the drug was embedded in a lipid matrix which was insoluble in an aqueous medium (Table XII).
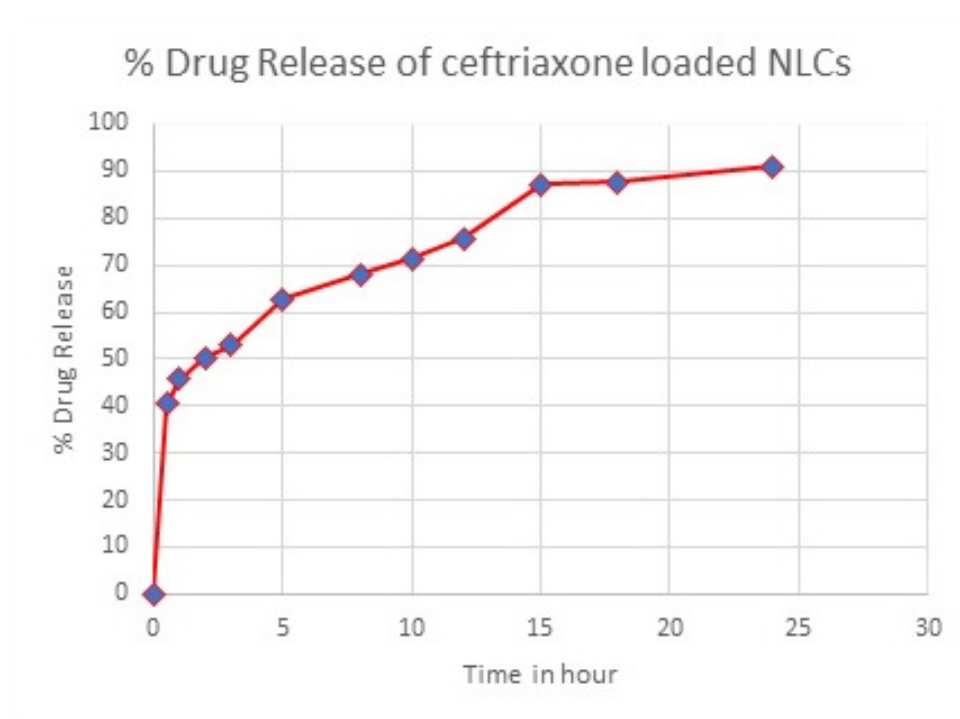
FIGURE 6 - *In vitro* % drug release from ceftriaxone loaded NLCs.

TABLE XII - Result of in *vitro* release kinetics studies

Formulation	First Order		Zero Order		Higuchi		Korsemeyer Peppas	
	K	R^2	K	R^2	K (Higuchi constant)	R^2	K and n	R^2
Optimized Formulation of ceftriaxone loaded NLCs	0.0365	0.9712	2.2218	0.9227	0.1276	0.9829	K= 1.6502 n=0.2181	0.9729

In vitro permeability studies using parallel artificial membrane permeability assay

PAMPA assay can be used as an alternative to find and compare the permeability of different formulations which can be used as an accompaniment for passive transport of the same through the blood brain barrier. Therefore, to establish a simulated membrane as BBB, lipids like porcine polar brain lipid (PBL) is used, but this process has its own limitations and can never be exactly as the biological BBB, as the composition of the brain varies from species to species, age factors, and other factors. The graph plotted between the concentration of ceftriaxone loaded NLCs transported versus time indicates that the system follows a non-steady state of diffusion (Figure 7).

The curve shows that $C_{acceptor}$ approaches asymptotically indicating that the drug concentration in the receiver chamber will increase exponentially. PAMAP-BBB assay method has emerged as a new technique to find out the passive permeability of drug candidates and their formulations. In the literature, it has been stated that if the permeability value of a substance was greater than 4×10^{-6} cm/s then those are permeable through BBB. Pe value of ceftriaxone solution in PAMPA-BBB assay was found to be 0.2×10^{-6} cm/s, designating that it is impermeable through uninflamed meninges and hence ceftriaxone was suitable to encapsulate into NLCs. The permeability of ceftriaxone loaded NLCs was found to be enhanced that is 5.06×10^{-6} cm/s, confirming that the permeability of NLCs of ceftriaxone was increased 28 times than the aqueous solution of ceftriaxone.
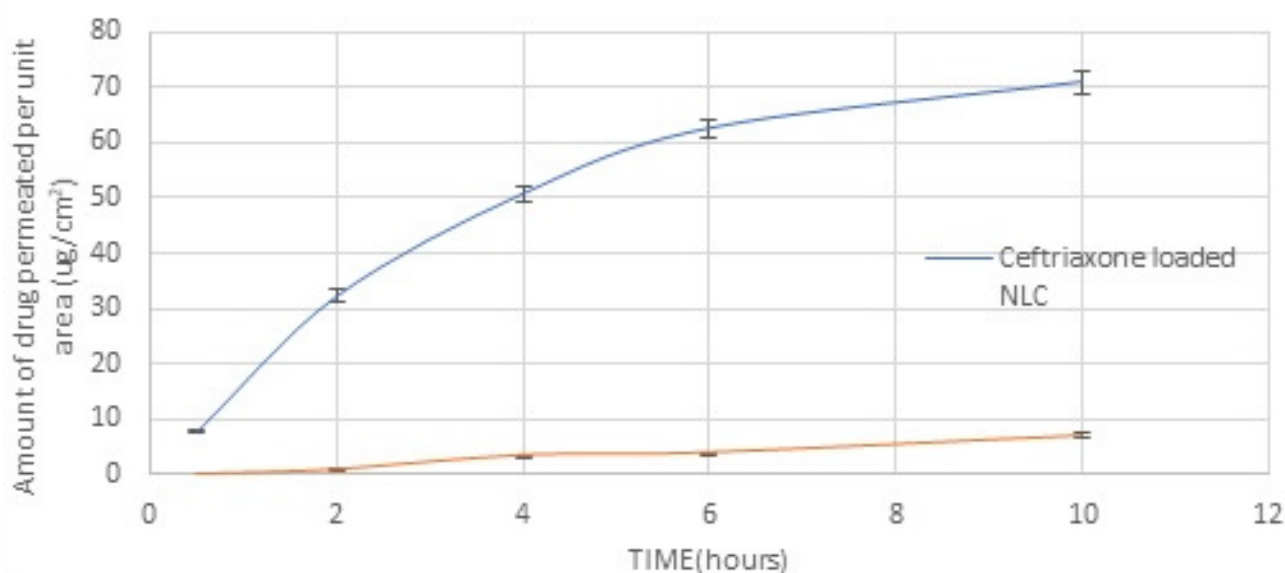
FIGURE 7 - Concentration of ceftriaxone loaded NLCs transported through PBL membrane versus time.

Biodistribution of ceftriaxone loaded NLCs

The concentration of ceftriaxone in brain and blood plasma was calculated after 8h of intravenous administration for initial biodistribution assessment. The result of the concentration of drug in plasma and blood is given in Table XIII. The ratio of drug concentration between brain and plasma for ceftriaxone loaded NLCs was calculated to be 0.29 and for ceftriaxone solution, the ratio was 0.02

TABLE XIII - Biodistribution of drug loaded NLCs

formulation	Blood Plasma(µg/ml)	Brain(µg/0.5g)	[Brain]/[Plasma]
NLCs ceftriaxone	25.5±1.1	7.49±0.24	0.29
Ceftriaxone solution	31.95±1.2	0.94±0.02	0.02

n=4

A significant difference existed between the concentration of drug present in rat brain tissue after administration of ceftriaxone solution and after administration of drug loaded NLCs, at $p<0.05$ (ANOVA). Therefore, it was concluded that the permeability of the drug through uninflamed meninges increases when the drug was embedded in nanostructured lipid carriers. Even with 44.32% entrapment of the drug in NLCs we were able to enhance the biodistribution of ceftriaxone 7.9 times compared to the biodistribution of the drug after administration of ceftriaxone solution.

Structural characterization of optimized formulation

Differential scanning calorimeter and X-ray diffraction technique are employed to analyze the structure of the optimized lyophilized NLCs loaded with ceftriaxone.

Differential scanning calorimeter Analysis

The DSC analysis had shown the endothermic peak of pure lipid glyceryl monostearate at 68.23^0C, which, represented the melting peak of the solid lipid (Figure 8). For pure ceftriaxone, it was found to have a peak at 132.70^0C. The peak value of glyceryl monostearate decreased to 57.81^0C when the drug and the liquid lipid were added to it and in the admixture, another melting peak was also noted at 131.39^0C. In the case of freeze dried NLCs one major endothermic peak was found at 58.73^0C which shows that the drug was completely covered by lipids.
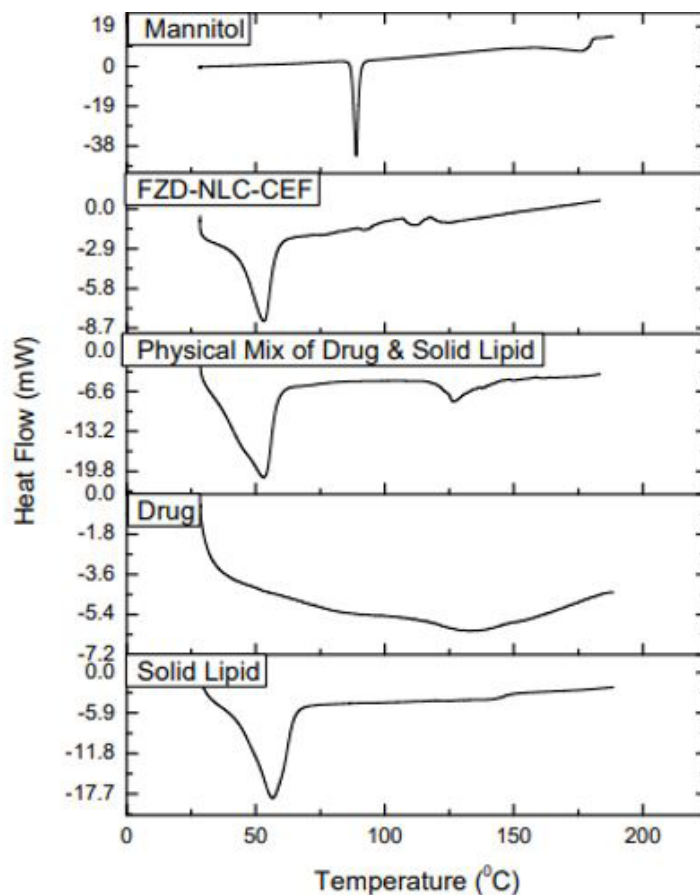
FIGURE 8 - DSC thermograms of mannitol, solid lipid; drug; the physical admixture of drug, solid lipid, and liquid lipid; FZD-NLC (Freeze-dried NLC of optimized formulation).

The DSC of FZD NLCs showed that the peak of the drug was almost missing revealing that the drug has fully dispersed in the lipid. The decrease in the melting points of the FZD NLCs of ceftriaxone compared to that of solid lipid suggested that the particle size of the freeze dried NLCs has been reduced to nanometric size as attributed to the Kelvin effect given by Thomson equation and the results of DSC suggest the formation of imperfection in the crystal structure of the prepared NLCs.

X-ray diffraction

The study of the crystalline orientation of drug (Ceftriaxone sodium), solid lipid glyceryl monostearate, the physical admixture of the drug, solid lipid and liquid lipid and freeze dried NLCs of optimized formulation was done by X-ray diffraction technique (Table XIV, Figure 9).
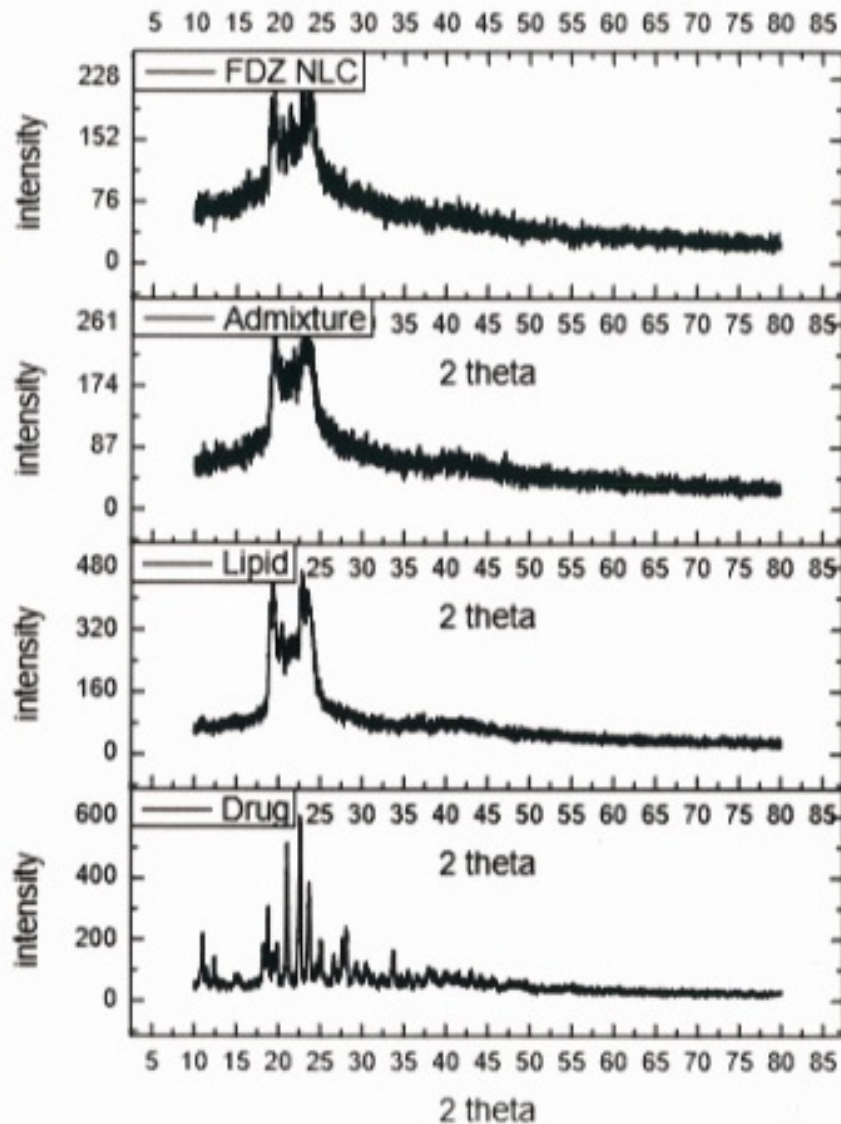
FIGURE 9 - Showing XRD of drug, solid lipid, the physical admixture of drug, solid lipid and liquid lipid, and Freeze-dried NLC of the optimized formulation.

Pure Ceftriaxone sodium exhibited large numbers of discrete sharp and robust peaks at the 2θ values mentioned in Table XIV exhibited the high crystalline structure of the drug (degree of crystallinity was found to be 83%). The full-width half maximum (FWHM) values of the studied samples depict the crystal size and stress-strain gathered in the material during the process of size reduction. The FWHM values are inversely related to the particle size and sharper XRD peaks denote small values of FWHM; for the pure drug in crystalline form, the FWHM value is found to be less than 1, as has been mentioned in Table XIV.

The value of FWHM to the corresponding 2theta is less than 1 indicates the drug's crystalline nature and suggests that the drug has not been subjected to any stress. The intensity and the number of peaks of the solid lipid were less than those of the drug and the corresponding FWHM values show that its amorphous nature predominates. The number of peaks and intensity further decrease for the physical admixture of the drug, solid lipid, and liquid lipid, but the XRD pattern of the optimized freeze dried NLCs shows that there are fewer number and widened peaks related to the pure drug and the solid lipid revealing that the crystalline

structures have been converted into amorphous form (Figure 9). The nature of the observed peaks depicts that in NLC formulation, ceftriaxone is molecularly solubilized (dispersed) forming the lipid matrix. The FWHM values (1.95 and 2.88) and wide peaks of the freeze dried NLCs are evidence that the system was subjected to stress to reduce the particle size suggesting structural disorder.

TABLE XIV - Data of X-ray diffraction analysis

Drug		Solid lipid		Physical admixture of drug and lipids		Freeze dried NLC	
2-theta	FWHM (deg)	2-theta	FWHM (deg)	2-theta	FWHM (deg)	2-theta	FWHM (deg)
11.036	0.23	19.06	0.45	18.99	0.28	19.12	1.95
11.52	0.21	19.55	0.48	19.44	0.63	23.71	2.88
12.44	0.20	20.68	3.76	20.35	2.1		
18.32	0.34	22.91	0.35	23.56	1.97		
18.81	0.27	23.93	1.53				
19.90	0.64						
21.12	0.29						
22.68	0.29						
23.69	0.29						
25.09	0.29						
26.66	0.28						
28.15	0.65						
29.36	0.48						
30.55	0.45						
33.76	0.34						

FWHM -full width half maximum of XRD peak

CONCLUSION

Ceftriaxone loaded NLCs were formulated with the purpose to overcome the permeability problem of ceftriaxone through uninflamed meninges. The theoretical solubility parameter calculation and the experimental results suggested that glyceryl monostearate and Capryol90 were the optimal lipids compared to the other investigational lipids. These two lipids were found to be compatible with the drug and the thermal events suggested that the solid lipid and the liquid lipids were to be used in a ratio of 70:30 used respectively. NLCs ceftriaxone were formulated and optimized using Box Behnken design. The optimized formulation was lyophilized, and the particle size was 130.58nm±6.54, PDI was 0.28±0.089, zeta potential -29.05mV±4.56, entrapment efficiency was 44.32%±5.89 and drug loading was 8.10%±0.8. The in vitro release kinetics was found to best fit slow first order and Higuchi kinetic model which confirms that the release followed the diffusion mechanism. Further, when the release data fitted to Korsmeyer-Peppas equation, which showed that the release exponent(n) was 0,22 suggesting Fickian type of diffusion

as the drug was embedded in a liquid matrix which was insoluble in an aqueous medium. The in vitro permeability studies using parallel artificial membrane permeability assay using procine polar brain lipid and the permeability of ceftriaxone loaded NLCs was found to be 5.06×10^{-6} cm/s which was 28 times greater compared to that of aqueous solution of ceftriaxone. Further the biodistribution of ceftriaxone loaded NLCs was found to be 7.49 µg/0.5g of brain after 8h of IV administration whereas for ceftriaxone solution biodistribution was found to be 0.94µg/0.5g of brain. It was found that permeability ceftriaxone loaded NLCs, even with 44.32 % entrapment of the drug in NLCs, we were able to enhance the biodistribution of ceftriaxone 7.9 times compared to the biodistribution of the drug after administration of ceftriaxone solution.

DSC and XRD study suggest the formation of imperfection in the crystal structure of the prepared NLCs and suggest that the drug holding capacity of NLCs is enhanced as the structure is nor crystalline. The research paves a new path which increases the permeability of hydrophilic drugs through uninflamed meninges preventing the development of multidrug resistance in infectious disease as well ensures effectiveness of the drug for better treatment of infectious disease during the early and recovery stage.

ACKNOWLEDGMENT

CONFLICT OF INTEREST

Authors have no conflict of interest.

REFERENCE

Alam T, Pandit J, Vohora D, Aqil M, Ali A, Sultana Y. Optimization of nanostructured lipid carriers of lamotrigine for brain delivery: in vitro characterization and in vivo efficacy in epilepsy. Expert Opin Drug Del. 2015;12(2):181-94.

Almousallam M, Moia C, Zhu H. Development of nanostructured lipid carrier for dacarbazine delivery. Int Nano Lett. 2015;5(4):241-8.

Ameeduzzafar Z, Ibrahim El-Bagory, Alruwaili NK, Mohammed HE, Javed A, Muhammad A, et al. Development of novel dapagliflozin loaded solid self-nanoemulsifying oral delivery system: Physiochemical characterization and in vivo antidiabetic activity. J Drug Deliv Sci Tec. 2019;54:101279.

Ameeduzzafar Z, Qumber M, Alruwaili NK, Bukhari SNA, Alharbi KS, Imam SS, et al. BBD-Based development of itraconazole loaded nanostructured lipid carrier for topical delivery: in vitro evaluation and antimicrobial assessment. J Pharm Innov. 2021;16(3):85-98.

Ameeduzzafar Z. Development of oral lipid based nano-formulation of dapagliflozin: optimization, in vitro characterization and *ex vivo* intestinal permeation study. J Oleo Sci. 2020;69(11):1389-1401.

Barra J, Lescure F, Doelker E, Bustamante P. The expanded Hansen approach to solubility parameters. Paracetamol and citric acid in individual solvents. J Pharm Pharmacol. 1997;49(7):644-51.

Cherubin CE, Eng RH, Norrby R, Modai J, Humbert G, Overturf G. Penetration of newer cephalosporins into cerebrospinal fluid. Rev Infect Dis. 1989;11(4):526-48.

Eedara BB, Rangnekar B, Doyle C, Cavallaro A, Das SC. The influence of surface active l-leucine and 1, 2-dipalmitoyl-sn-glycero-3-phosphatidylcholine (DPPC) in the improvement of aerosolization of pyrazinamide and moxifloxacin co-spray dried powders. Int J Pharm. 2018;542(1-2):72-81.

Emmerson AM, Lamport PA, Reeves DS, Bywater MJ, Holt HA, Wise R, et al. The in vitro antibacterial activity of ceftriaxone in comparison with nine other antibiotics. Curr Med Res Opin. 1985;9(7):480-93.

Feng F, Zheng D, Zhang D, Duan C, Wang Y, Jia L, et al. Preparation, characterization and biodistribution of nanostructured lipid carriers for parenteral delivery of bifendate. J Microencapsul. 2011;28(4):280-5.

Gartziandia O, Herran E, Pedraz JL, Carro E, Igartua M, Hernandez RM. Chitosan coated nanostructured lipid carriers for brain delivery of proteins by intranasal administration. Colloid Surf B. 2015;134:304-13.

Gonzalo R, Laura TA, Fanny d'Orlyé, Anne V. Electrophoretic methods for characterizing nanoparticles and evaluating their bio-interactions for their further use as diagnostic, imaging, or therapeutic tools. Colin F. Poole, editor. In Handbooks in Separation Science, Capillary Electromigration Separation Methods. Elsevier. 2018;397-421.

Graverini G, Piazzini V, Landucci E, Pantano D, Nardiello P, Casamenti F, et al. Solid lipid nanoparticles for delivery of andrographolide across the blood-brain barrier: in vitro and in vivo evaluation. Colloid Surf B. 2018;161:302-13.

Hancock BC, York P, Rowe RC. The use of solubility parameters in pharmaceutical dosage form design. Int J Pharm. 1997;148(1):1-21.

Hansen CM. The three-dimensional solubility parameters-key to paint component affinities, solvents, plasticizers, polymers and resins. J Paint Technol. 1967;39:104-117.

Hao J, Fang X, Zhou Y, Wang J, Guo F, Li F, et al. Development and optimization of solid lipid nanoparticle formulation for ophthalmic delivery of chloramphenicol using a Box-Behnken design. Int J Nanomed. 2011;6:683-92.

Huttunen K, Rautio J. Prodrugs-an efficient way to breach delivery and targeting barriers. Curr Top Med Chem. 2011;(18):2265-87.

Jayanthi B, Sarojini S, Manikandan M, Manna PK. Application of central composite design based on response surface methodology for optimization of extended release aceclofenac microparticles. Eur J Pharm Med Res. 2016;3(10):163-172.

Kasongo KW, Müller RH, Walker RB. The use of hot and cold high pressure homogenization to enhance the loading capacity and encapsulation efficiency of nanostructured lipid carriers for the hydrophilic antiretroviral drug, didanosine for potential administration to paediatric patients. Pharm Dev Technol. 2012;17(3):353-62.

Kasongo WA, Pardeike J, Müller RH, Walker RB. Selection and characterization of suitable lipid excipients for use in the manufacture of didanosine-loaded solid lipid nanoparticles and nanostructured lipid carriers. J Pharm Sci. 2011;100(12):5185-96.

Kovacevic A, Savic S, Vuleta G, Mueller RH, Keck CM. Polyhydroxy surfactants for the formulation of lipid nanoparticles (SLN and NLC): effects on size, physical stability and particle matrix structure. Int J Pharm. 2011;406(1-2):163-72.

Krevelen DV. Cohesive properties and solubility. In: Properties and Polymers. 2009;189-225.

Lakshmi KS, Ilango K, Nithya MN, Balaji S, KibeVictor DW, Sathish KV. Spectrophotometric methods for the estimation of ceftriaxone sodium in vials. Int J Pharm Sci. 2009;1:22-5.

Li XW, Lin XH, Zheng LQ, Yu L, Mao HZ. Preparation, characterization, and in vitro release of chloramphenicol loaded solid lipid nanoparticles. J Disper Sci Technol. 2008;29(9):1214-21.

Li Y, Taulier N, Rauth AM, Wu XY. Screening of lipid carriers and characterization of drug-polymer-lipid interactions for the rational design of polymer-lipid hybrid nanoparticles (PLN). Pharm Res. 2006;23(8):1877-87.

Mahdi WA, Bukhari SI, Imam SS, Alshehri S, Zafar A, Yasir M. Formulation and optimization of butenafine-loaded topical nano lipid carrier-based gel: characterization, irritation study, and anti-fungal activity. Pharmaceutics. 2021;13(7):1087.

Mandell GL, Sande MA. Antimicrobial agents: penicillins, cephalosporins, and other beta-lactam antibiotics. Goodman & Gilman's The pharmacologic basis of therapeutics, 9th ed. New York: McGraw-Hill, Health Professions Division. 1996:1073-101.

McDaid FM, Barker SA, Fitzpatrick S, Petts CR, Craig DQ. Further investigations into the use of high sensitivity differential scanning calorimetry as a means of predicting drug–excipient interactions. Int J Pharm. 2003;18;252(1-2):235-40.

Mohammed HE, Mohammed E, Khaled S, Ahmed FA, Naveed A, Ameeduzzafar Z, Hussein ME. Development and machine-learning optimization of mucoadhesive nanostructured lipid carriers loaded with fluconazole for treatment of oral candidiasis. Drug Dev Ind Pharm. 2021;47(2):246-258.

Nasiri M, Azadi A, Zanjani MRS, Hamidi M. Indinavir-loaded nanostructured lipid carriers to brain drug delivery: optimization, characterization and neuropharmacokinetic evaluation. Curr Drug Deliv. 2019;16(4):341-354.

Nau R, Prange HW, Muth P, Mahr G, Menck S, Kolenda H, et al. Passage of cefotaxime and ceftriaxone into cerebrospinal fluid of patients with uninflamed meninges. Antimicrob Agents Chemother. 1993;37(7):1518-24.

Neves AR, Queiroz JF, Reis S. Brain-targeted delivery of resveratrol using solid lipid nanoparticles functionalized with apolipoprotein E. J Nanobiotechnol. 2016;14(1):1-1.

Padhi S, Mazumder R, Bisth S. Development and application of lipid nanotechnology on infectious diseases of CNS-current scenario. Ind J Pharm Educ Res. 2019;53(3):355-65.

Pani NR, Nath LK, Acharya S, Bhuniya B. Application of DSC, IST, and FTIR study in the compatibility testing of nateglinide with different pharmaceutical excipients. J Therm Anal Calorim. 2012;108(1):219-26.

Park SY, Kang Z, Thapa P, Jin YS, Park JW, Lim HJ, et al. Development of sorafenib loaded nanoparticles to improve oral bioavailability using a quality by design approach. Int J Pharm. 2019;566:229-38.

Patil GB, Surana SJ. Fabrication and statistical optimization of surface engineered PLGA nanoparticles for naso-brain delivery of ropinirole hydrochloride: in-vitro–ex-vivo studies. J Biomat Sci-Polym E. 2013;24(15):1740-56.

Rowe R, Interaction of lubricants with microcrystalline cellulose and anhydrous lactose — a solubility parameter approach. Int J Pharm. 1998;41(3):223–226.

Salem DS, Sliem MA, El-Sesy M, Shouman SA, Badr Y. Improved chemo-photothermal therapy of hepatocellular carcinoma using chitosan-coated gold nanoparticles. J Photochem Photobiol B. 2018;182:92-99.

Salunkhe SS, Bhatia NM, Kawade VS, Bhatia MS. Development of lipid based nanoparticulate drug delivery systems and drug carrier complexes for delivery to brain. J Appl Pharm Sci. 2015;5(5):110-29.

Santaguida S, Janigro D, Hossain M, Oby E, Rapp E, Cucullo L. Side by side comparison between dynamic versus static models of blood–brain barrier in vitro: a permeability study. Brain Res. 2006;1109(1):1-3.

Shah A, Yameen MA, Fatima N, Murtaza G. Chemical synthesis of chitosan/silver nanocomposites films loaded with moxifloxacin: their characterization and potential antibacterial activity. Int J Pharm. 2019;561:19-34.

Shah M, Agrawal Y. High throughput screening: an in silico solubility parameter approach for lipids and solvents in SLN preparations. Pharm Dev Technol. 2013;18(3):582-90.

Shah M, Agrawal YK, Garala K, Ramkishan A. Solid lipid nanoparticles of a water-soluble drug, ciprofloxacin hydrochloride. Indian J Pharm Sci. 2012;74(5):434.

Subedi RK, Kang KW, Choi HK. Preparation and characterization of solid lipid nanoparticles loaded with doxorubicin. Eur J Pharm Sci. 2009;37(3-4):508-13.

Tajes M, Ramos-Fernández E, Weng-Jiang X, Bosch-Morato M, Guivernau B, Eraso-Pichot A, et al. The blood-brain barrier: structure, function and therapeutic approaches to cross it. Mol Membr Biol. 2014;31(5):152-67.

Tsai MJ, Wu PC, Huang YB, Chang JS, Lin CL, Tsai YH, et al. Baicalein loaded in tocol nanostructured lipid carriers (tocol NLCs) for enhanced stability and brain targeting. Int J Pharm. 2012;423(2):461-70.